Article

Toward Achieving Single-Molecule White Electroluminescence from Dual Emission of Fluorescence and Phosphorescence

Hao Chen, Yihua Deng, Xiangyu Zhu, Lu Wang, Lei Lv, Xiaoxi Wu, Zijie Li, Qinqin Shi, Aidong Peng, Qian Peng,* Zhigang Shuai, Zujin Zhao,* Huajie Chen, and Hui Huang*

Cite This: *Chem. Mater.* 2020, 32, 4038−4044

Read Online

ACCESS | Metrics & More | Article Recommendations | Supporting Information

ABSTRACT: White organic light-emitting diodes (WOLEDs) are of great value in daily life. However, the organic white-emissive single molecules in OLEDs are rare. Herein, we report a group of carbazolyl derivatives containing thiophene (PhCz-S), selenophene (PhCz-Se), and tellurophene (PhCz-Te). Through modulating the chalcogen atom, the promoted intersystem crossing brings room-temperature phosphorescence. Moreover, PhCz-Se exhibits Commission Internationale de l'Eclairage (CIE) coordinates of (0.30, 0.29) in OLEDs measured at 4 V, which is the first example of the single-molecule WOLEDs combined with dual emission from singlet and triplet states. Also, PhCz-Te realized WOLEDs in a single emission layer at CIE coordinates of (0.34, 0.33). The theoretical and experimental results clearly show that the adjustment of heavy atoms exerts influence on the luminescent properties, which provides a new strategy for designing single-molecule WOLEDs.
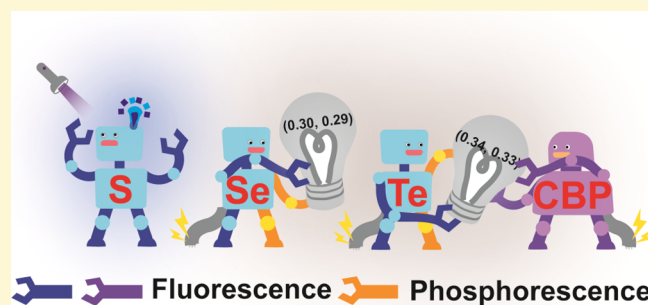
1. INTRODUCTION

Organic light-emitting diodes (OLEDs) are undergoing rapid progress because of their advantages of flexibility, low cost, light weight, and solution processibility.[1−3] Among them, white OLEDs (WOLEDs) are of great importance in practical applications. Since the first WOLED that was developed in 1995,[4] high EL efficiencies have been achieved via employing blends as emissive layers.[5−9] However, WOLEDs based on blend systems suffered from bias-dependent electroluminescence (EL) spectra and intrinsic phase separation during long-term device operation.[10−14] Therefore, developing single-molecule white EL materials is attracting much attention.

To date, several important strategies have been developed to realize single-molecule white EL, such as the formation of excimers,[15−19] exciplexes,[20−23] aggregation,[24,25] and so forth. However, most of white EL originated from electrofluorescence; so the maximal internal quantum efficiency is limited to 25%.[26] To break this limit, triplet emitters were introduced, leading to phosphorescent OLEDs.[27−29] Since the reporting of first single-dopant phosphorescent WOLED,[30] the materials, emitting modes, and mechanisms have become rich and colorful. Generally, metallic elements are introduced into luminogens to promote spin−orbit coupling (SOC) through heavy atom effect, resulting in electrophosphorescence. However, the high cost of heavy metals and difficulty of tuning fluorophore hosts and phosphors severely limited the development of phosphorescence materials. Thus, developing metal-free electrophosphorescent materials and exploring novel strategies for single-molecule WOLEDs are in high demand.[31,32]

Herein, we report the first example of metal-free single-molecule white EL with dual emission of fluorescence and phosphorescence. Three analogous materials (PhCz-S, PhCz-Se, and PhCz-Te) were synthesized through Stille coupling in good yields to investigate the heteroatom effects. The replacement of S with Se and Te atoms yielded room-temperature phosphorescence (RTP) because of heavy atom effects. Impressively, PhCz-Se generated white EL upon singlet and triplet harvesting in a single molecule, whereas PhCz-Te realized single emitting layer WOLEDs when doped into OLEDs. Thus, the fluorescence and phosphorescence properties were systematically tuned by simply tuning the chalcogen atoms, which provided a new route to achieve WOLEDs.

2. EXPERIMENTAL SECTION

2.1. Synthesis and Characterization. Initial reactants such as 9H-carbazole, 4-iodobenzoyl chloride, and acetyl chloride were commercially available, which were used directly without further purification. Three compounds (PhCz-S, PhCz-Se, and PhCz-Te)

Table 1. Photophysical Properties of PhCz-S, PhCz-Se, and PhCz-Te

compound	$\lambda_{abs}{}^a$ (nm)	$E_g{}^a$ (eV)	HOMO^b (eV)	LUMO^b (eV)	$\lambda_{em}{}^c$ (nm)	$\tau_f{}^d$ (ps)	$\tau_p{}^e$ (μs)	$\Phi_s{}^f$ (%)	$\Phi_c{}^g$ (%)
PhCz-S	285, 324	3.24	−6.06	−2.95	466	1100		4.90	0.99
PhCz-Se	288, 330	3.08	−6.03	−2.96	438, 590	285.6	113.1	3.89	1.56
PhCz-Te	288, 323	3.04	−5.65	−2.98	510, 650	59.9	12.2	1.46	0.67

^{a}UV−vis absorption peaks and band gaps in films at room temperature. $E_g = 1240/\lambda_{off}$. ^{b}Experimental data obtained by CV in anhydrous acetonitrile solution, calculated from $E_{HOMO/LUMO} = -(E^{ox/red} + 4.44)$ eV. ^{c}Emission peaks. ^{d}Fluorescence lifetime in the crystalline state. ^{e}Phosphorescence lifetime in the crystalline state. ^{f}Photoluminescent quantum yields in tetrahydrofuran solution (5.0×10^{-5} M). ^{g}Photoluminescent quantum yields in the crystalline state at room temperature.

were synthesized via Stille coupling reactions (Scheme S1). More detailed synthesis procedures are described in the Supporting Information.

Ultraviolet−visible (UV−vis) absorption spectra were measured on a Gary 60 UV−vis spectrophotometer. The other photophysical properties were experimented on a FLS980 spectrometer. The absolute photoluminescence (PL) quantum yields were measured on a FLS980 spectrometer equipped with an integrating sphere and calculated from the blank and sample emission measurement.

2.2. Computation Methodology. Geometry optimizations were performed by the restricted density functional theory (DFT) for the ground states and unrestricted DFT for the triplet excited states. We used B3LYP functional with ECP basis set Lanl2dz for heavy atom Te and 6-31g(d) for the other atoms in the optimizations. The solid phase environment is considered by using the quantum mechanics and molecular mechanics approach, that is, the solid-phase system is treated as a cluster using the two-layer ONIOM method (1 molecule for quantum mechanism and 35 molecules for molecular mechanism calculations). Time-dependent DFT (TD−DFT) with Tamm−Dancoff approximation was applied for calculating the excitation energies in the same level.

2.3. Device Fabrication and Measurement. Device fabricating procedures can be found in the Supporting Information. The device characterizations were carried out at room temperature under ambient conditions without encapsulation, except the spectrum collection process. EL spectra were taken by an optical analyzer, Photo Research PR745. Current density and luminance versus driving voltage characteristics were measured by a Keithley 2400 system and a Konica Minolta chromameter CS-200, respectively. External quantum efficiencies were calculated by assuming that the devices were Lambertian light sources.

3. RESULTS AND DISCUSSION

3.1. Electrochemical and Photophysical Properties. The electrochemical properties of the three compounds (PhCz-S, PhCz-Se, and PhCz-Te) were studied by cyclic voltammetry (CV) as shown in Figure S9. The highest occupied molecular orbital (HOMO) and lowest unoccupied molecular orbital (LUMO) data are summarized in Table 1. It is obvious that the HOMO energy levels continuously increase when chalcogen atoms change from thiophene to selenophene and tellurophene, which are −6.06, −6.03, and −5.65 eV for PhCz-S, PhCz-Se, and PhCz-Te, respectively. Moreover, the LUMO energy levels continuously decrease from PhCz-S (−2.95 eV) to PhCz-Se (−2.96 eV) and PhCz-Te (−2.98 eV). As a result, the order of the band gaps is PhCz-Te < PhCz-Se < PhCz-S, consistent with the data of reported literature.[33]

Figure 1B shows the UV−vis absorption of PhCz-S, PhCz-Se, and PhCz-Te, which exhibit similar absorption profiles with two peaks in solution. The absorption peaks in thin films slightly red shift 4, 7, and 3 nm in comparison to the three compounds in solution (Figure S10), which suggests moderate packing in the solid state because of their twisted structures.[34]

Figure S11 shows the PL spectra of the three compounds in different solvents. While in the crystalline state (Figure 2A),
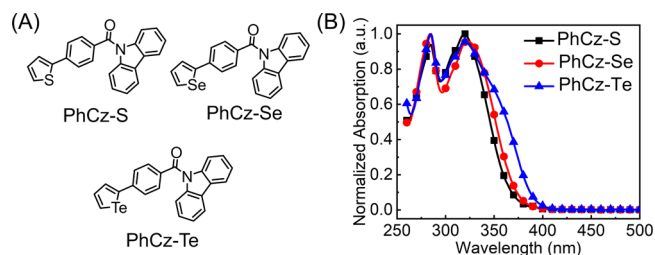

Figure 1. (A) Structure of three compounds. (B) UV−vis absorption in chloroform.

PhCz-S only exhibits one emission peak at 450 nm (excited at 408 nm) with a short lifetime of 1.1 ns at room temperature. In comparison, both PhCz-Se and PhCz-Te exhibit two emission peaks, which can be attributed to fluorescence and phosphorescence. The fluorescence emission with picosecond order lifetimes is located at a short wavelength, whereas the phosphorescence emission is located at a long wavelength. The emission peak at 590 nm for PhCz-Se possesses a lifetime of 113.1 μs, whereas the peak at 650 nm for PhCz-Te exhibits 12.2 μs lifetime under an ambient condition. The low photoluminescent quantum yields of the three compounds in crystal are likely due to the oxygen quenching of the triplet state, resulting in lower values than the materials are capable of emitting.

Steady-state and transient spectroscopies of PhCz-Se and PhCz-Te at different temperatures were performed to understand the property of long-lived luminescence (Figures 2B,C and S12). The lifetimes for PhCz-Se and PhCz-Te both increase slightly as the temperature decreases to 77 K (Table S1) because of the suppression of the nonradiative transition and vibrational relaxation, which rules out the possibility of delayed fluorescence.[35] Therefore, the emission peaks are reasonably ascribed to RTP. Furthermore, the phosphorescence proportion of emission in PhCz-Te is larger than that in PhCz-Se, which indicates that tellurium promotes more efficient intersystem crossing (ISC).

3.2. Crystal Structures of Compounds. In order to understand the relationship between the photophysical properties and intermolecular interaction, single crystals of the three molecules were cultivated for X-ray diffraction. Figure S13 and Table S2 show the single-crystal structures and data of the three molecules. In PhCz-S and PhCz-Se, the heteroatoms (S and Se) and carbonyl are located at different sides. However, PhCz-Te possesses two kinds of crystal structures. In one type, tellurium and carbonyl are at the same side (PhCz-Te inner), whereas tellurium and carbonyl are at different sides in the other type (PhCz-Te outer).

As shown in Figure 3, all single-crystal structures contain various intermolecular interactions. The C−H···π short intermolecular contacts are present in PhCz-S (2.758 and
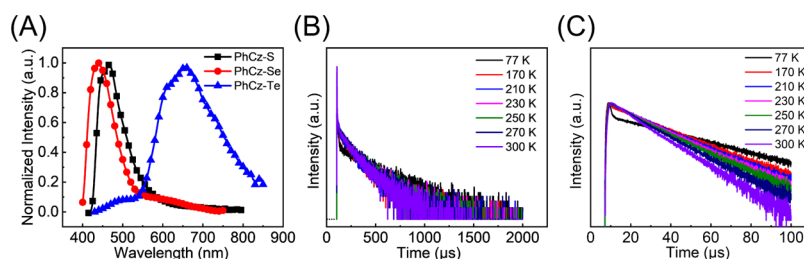
Figure 2. (A) Steady-state PL spectra of crystal PhCz-S (excited at 408 nm), PhCz-Se (excited at 384 nm), and PhCz-Te (excited at 410 nm). Time-resolved PL decay curves of (B) PhCz-Se and (C) PhCz-Te measured from 77 to 300 K.
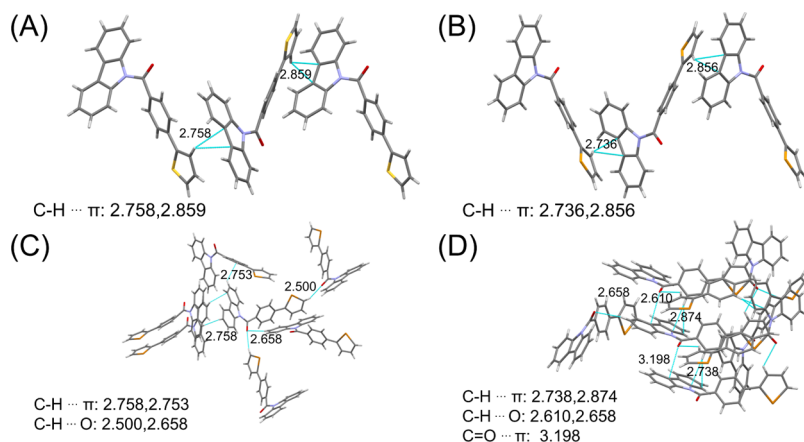

Figure 3. Intermolecular noncovalent interactions in single crystals of (A) PhCz-S, (B) PhCz-Se, (C) PhCz-Te-inner, and (D) PhCz-Te-outer.

2.859 Å) and PhCz-Se (2.736 and 2.856 Å). In PhCz-Te, there exist more short contact interactions than PhCz-S and PhCz-Se, such as C−H⋯π (2.753 and 2.758 Å) and C−H⋯O (2.500 and 2.658 Å) in PhCz-Te inner and C−H⋯π (2.738 and 2.874 Å), C−H⋯O (2.610 Å and 2.658 Å), and C=O⋯π (3.198 Å) in PhCz-Te outer. The X−X (X for N, S, Se, or Te) distances in dimers can be found in Figure S14. Note that the shortest Te−Te interaction indicates the closest packing of PhCz-Te (Figure S15), which suggests that PhCz-Te may possess the strongest phosphorescence intensity.[36] At the same time, the large dihedral angle θ between carbazole and benzoyl groups of PhCz-Te (Figure S16) brings the spatial separation of HOMO and LUMO, which can narrow the energy gap between S_1 and T_1 (ΔE_{ST}).[34] According to the PL spectra at 77 K (Figure S12), PhCz-Te possesses lower ΔE_{ST} of 0.67 eV than PhCz-Se of 0.98 eV, which facilitates the ISC process. All factors favoring triplet excitons in PhCz-Te lead to a high phosphorescence intensity.

3.3. Theoretical Calculations. To further understand the photophysical differences of the three compounds, quantum calculations were performed by DFT and TD-DFT with Tamm−Dancoff approximation. The computational model and details can be found in the Supporting Information for the compounds in the solid phase (Figure S17). First, the theoretically optimized molecular geometries at the ground state and the experimental single-crystal structure of PhCz-S (Table S3) are in good agreement, indicating the reliability of the computational model and the theory approach adopted here. Second, the calculated absorption bands are 343 nm for PhCz-S, 360 nm for PhCz-Se, and 367/342 nm for PhCz-Te (Table S4), which well reproduced the experimental values in Table 1. Seeing the transition properties and frontier orbital characters in Table S4 and Figure S18, the absorption peak can

be reasonably assigned to the twisted intramolecular charge transfer (CT) between carbazole and the other moieties.[37]

$$k_{ISC} \propto |\langle S|\hat{H}_{SOC}|T\rangle|^2 \exp(-\Delta E_{ST}^2) \qquad (1)$$

As seen from eq 1, the energy gap and SOC are two important factors for the efficient ISC between the singlet and triplet states to induce RTP.[38,39] The calculated energy gaps and SOC constants (ξ) between the involved singlet and triplet states of PhCz-S, PhCz-Se, and PhCz-Te are depicted in Figure 4 based on the optimized T_1 geometry for the three compounds in the solid phase. As we speculated, $S_1 \rightarrow T_2$ is a very important ISC process to generate triplet from singlet
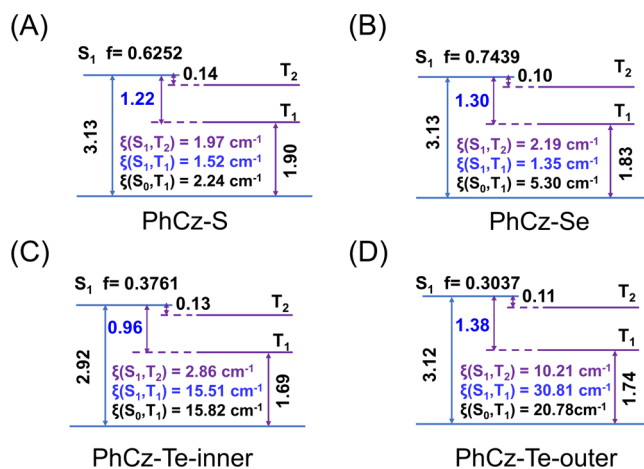

Figure 4. Calculated energy gaps (eV) and SOC constants between S_1, T_n, and S_0 based on the optimized T_1 geometry for (A) PhCz-S, (B) PhCz-Se, (C) PhCz-Te-inner, and (D) PhCz-Te-outer.

states because of its small energy gap for the three compounds. From PhCz-S to PhCz-Te, the energy gap between S_1 and T_2 is decreased and the SOC is increased, both of which can facilitate the conversion from singlet to triplet states.[40,41] From the frontier orbitals and transition properties of the low-lying excited states in Table S5 and Figure S19 in the Supporting Information, it can be seen that the S_1 states exhibit hybrid CT and localization excitation (LE) nature, and the T_2 states show an obvious CT feature, whereas the T_1 states are typical LE.[42] Also seen from the components of molecular configuration in Table S5, the CT component is larger than the LE one in the S_1 state for PhCz-S and PhCz-Se. Therefore, the SOC constant between S_1 and T_2 is larger than that between S_1 and T_1 because of the larger difference of molecular configuration between S_1 and T_2 according to the El-Sayed rule for PhCz-S and PhCz-Se.[43] Differently, the heavy atom effect becomes the dominant factor to induce a much stronger SOC for PhCz-Te. Especially, ξ between T_1 and S_0 goes up sharply with heavier atom from sulfur (PhCz-S) to tellurium (PhCz-Te). All these can cause faster ISC, resulting in improved phosphorescent quantum efficiency and shorter phosphorescent lifetime, as seen in Table 1.[44] In addition, the excitation energies of T_1 from the S_0 state are decreased from PhCz-Se to PhCz-Te, which are consistent with the red shift of the phosphorescence experimentally measured in the same order in Figure 2A. Overall, the theoretically calculated results provide solid evidence for the experimental phenomena.

3.4. Investigation of WOLEDs. Considering the dual fluorescence–phosphorescence properties of PhCz-Se and PhCz-Te, they were used to construct OLED devices to examine their electroluminescent performance. PhCz-Se was employed in a single emission layer of device I–III with the configuration (Figure 5A) of ITO/HATCN (5 nm)/NPB (40

material, and 2,8-bis(diphenylphosphoryl)dibenzo[b,d]furan (PPF) or bis[2-(diphenylphosphino)phenyl] ether oxide (DPEPO) was used as the host matrix.

Figure 5B shows that the EL spectrum is consistent with the PL one, whereas the emission peak at around 440 nm is assigned to the fluorescence from S_1 and 590 nm peak is identical to that in RTP. As shown in Figure S20, the emission peaks remain unchanged when the dopant concentration and host material change, which excludes the formation of exciplex.[45] Excitons are formed in both PPF and PhCz-Se but return to the ground state in PhCz-Se, following the Förster resonant energy-transfer process. The 25% singlet excitons and 75% triplet excitons generated in the emitting layer can both be employed by PhCz-Se owing to efficient ISC, which exhibits two kinds of emissions, corresponding to fluorescence and phosphorescence, respectively.[46] In addition, the more the charges are injected from the electrode, the more triplet states are produced, which are quenched owing to the long lifetime, namely, triplet–triplet annihilation (TTA). Thus, when the current increased, the proportion of electrophosphorescence becomes smaller, whereas fluorescence turned to be stronger. With regard to OLEDs, the radiative decay from singlet and triplet excitons blend together to achieve cool white emission located at the Commission Internationale de l'Eclairage (CIE) coordinates (0.30, 0.29) measured at 4 V, which is the first single-molecule WOLED combining fluorescence and phosphorescence.

Furthermore, device IV with a configuration of ITO/ HATCN (5 nm)/TAPC (20 nm)/TcTa (5 nm)/CBP:5 wt % PhCz-Te (35 nm)/TmPyPB (55 nm)/LiF (1 nm)/Al (Figure 5C) was fabricated, with dipyrazino [2,3-f:2′,3′-h] quinoxaline 2,3,6,7,10,11-hexacarbonitrile (HATCN) adopted as the hole injection material, 1,1-bis[(di-4-tolylamino)phenyl]-cyclohexane (TAPC) as the hole-transporting material, 4,4′,4″-tri(N-carbazolyl)triphenylamine (TcTa) as the exciton-blocking material, and 1,3,5-tri[(3-pyridyl)-phen-3-yl]benzene (TmPyPB) as electron-transporting material.

As shown in the EL spectra (Figure 5D), the small emitting peak around 380 nm is ascribed to 4,4′-bis(carbazol-9-yl)biphenyl (CBP), which is excited by the recombination of holes migrated from TAPC and electrons from TmPyPB and functioned as the host to transfer energy to triplet energy level of the dopant. Compared with the PL spectrum of PhCz-Te in Figure 2A, the two main peaks can be ascribed to the emission from singlet and triplet excitons. Finally, they simultaneously contribute to the pure white EL with CIE coordinates (0.34, 0.33). However, device IV shows slightly the TTA process that is observed in devices I–III at a high operating voltage. We propose that the heavy atom effect of tellurium in PhCz-Te brings about faster ISC from T_1 to S_0. Thus, as the exciton density in the emission layer gets higher, the triplet excitons tend to emit phosphorescence rather than undergo TTA.

The luminance–voltage–current density (L–V–J) and current efficiency–luminance–power efficiency (CE–L–PE) characteristics of PhCz-Se-based devices I–III and PhCz-Te-based device IV are shown in Figures S21–S23, and the data are summarized in Table S6. All devices exhibit turn-on voltages (V_{on}) above 5 V. The PhCz-Se-based devices exhibit a maximum current efficiency of 0.28 cd A^{-1}, a maximum brightness of 148.9 cd m^{-2} (at 15.8 V), a maximum external quantum efficiency of 0.22% and a maximum power efficiency of 0.07 lm W^{-1}, whereas the parameters for device IV are 0.38 cd A^{-1}, 305.2 cd m^{-2} (at 13.4 V), 0.25%, and 0.11 lm W^{-1},
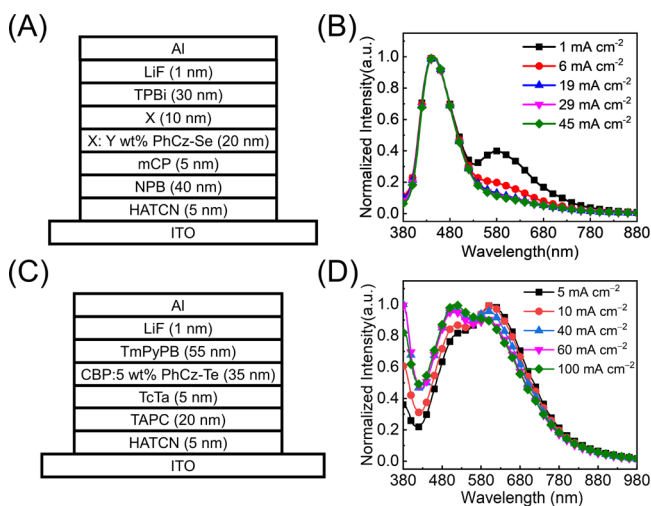

Figure 5. Structure of (A) devices I (X = PPF, Y = 5), II (X = PPF, Y = 10), III (X = S, Y = DPEPO), and (C) IV. EL spectra of devices (B) I and (D) IV.

nm)/mCP (5 nm)/X:Y wt % PhCz-Se (20 nm)/X (10 nm)/ TPBi (30 nm)/LiF (1 nm)/Al (X = PPF or DPEPO, Y = 5 or 10). N,N′-Di(1-naphthyl)-N,N′-diphenyl-(1,1′-biphenyl)-4,4′-diamine (NPB) acted as the hole-transporting material, 1,3-bis(N-carbazolyl)benzene (mCP) was the exciton-blocking material, 2,2′,2″-(1,3,5-benzinetriyl)-tris(1-phenyl-1-H-benzimidazole) (TPBi) was used as the electron-transporting

respectively. The average EL performance values of four devices were obtained from at least three devices, as listed in Table S7. The CIE coordinate spectra of four devices are shown in Figure S24, and all data can be repeated, which suggest the potential applications of PhCz-Se and PhCz-Te for WOLEDs.

4. CONCLUSIONS

In summary, a series of metal-free organic luminogens based on carbazole and heterocyclic ring with different chalcogen atoms were synthesized and characterized. Both PhCz-Se and PhCz-Te show dual fluorescence−phosphorescence emissive properties owing to heavy atom effects, which were supported by experimental and theoretical evidences. OLED devices based on PhCz-Se showed single-molecular white EL at an appropriate operating voltage, which is the first example of white EL originating from dual fluorescence and phosphorescence, whereas PhCz-Te-based ones exhibited white EL together with the host. This study demonstrates that varying the chalcogen atoms of heterocycles may be an efficient method for tuning the emissive properties of organic luminogens to achieve WOLEDs.

■ ASSOCIATED CONTENT

ⓈⒾ Supporting Information

The Supporting Information is available free of charge at https://pubs.acs.org/doi/10.1021/acs.chemmater.0c00710.

> Details of synthesis, measurements, crystal data, DFT calculations, and OLED fabrication and characterization (PDF)
> Crystal data for PhCz-S (CIF)
> Crystal data for PhCz-Se (CIF)
> Crystal data for PhCz-Te (CIF)

■ AUTHOR INFORMATION

Corresponding Authors

Qian Peng − *Key Laboratory of Organic Solids and Beijing National Laboratory for Molecular Science, Institute of Chemistry, Chinese Academy of Sciences, Beijing 100190, China;* ⓞ orcid.org/0000-0001-8975-8413; Email: qpeng@iccas.ac.cn

Zujin Zhao − *State Key Laboratory of Luminescent Materials and Devices, Guangdong Provincial Key Laboratory of Luminescence from Molecular Aggregates, South China University of Technology, Guangzhou 510640, China;* ⓞ orcid.org/0000-0002-0618-6024; Email: mszjzhao@scut.edu.cn

Hui Huang − *College of Materials Science and Opto-Electronic Technology & CAS Center for Excellence in Topological Quantum Computation & Key Laboratory of Vacuum Physics, University of Chinese Academy of Sciences, Beijing 100049, P. R. China;* ⓞ orcid.org/0000-0002-6102-2815; Email: huihuang@ucas.ac.cn

Authors

Hao Chen − *College of Materials Science and Opto-Electronic Technology & CAS Center for Excellence in Topological Quantum Computation & Key Laboratory of Vacuum Physics, University of Chinese Academy of Sciences, Beijing 100049, P. R. China*

Yihua Deng − *College of Materials Science and Opto-Electronic Technology & CAS Center for Excellence in Topological*

Quantum Computation & Key Laboratory of Vacuum Physics, University of Chinese Academy of Sciences, Beijing 100049, P. R. China; Key Laboratory of Environmentally Friendly Chemistry and Application of the Ministry of Education, and Key Laboratory for Green Organic Synthesis and Application of Hunan Province, College of Chemistry, Xiangtan University, Xiangtan 411105, China

Xiangyu Zhu − *State Key Laboratory of Luminescent Materials and Devices, Guangdong Provincial Key Laboratory of Luminescence from Molecular Aggregates, South China University of Technology, Guangzhou 510640, China*

Lu Wang − *Department of Chemistry and MOE Key Laboratory of Organic Optoelectronics and Molecular Engineering, Tsinghua University, Beijing 100084, China*

Lei Lv − *College of Materials Science and Opto-Electronic Technology & CAS Center for Excellence in Topological Quantum Computation & Key Laboratory of Vacuum Physics, University of Chinese Academy of Sciences, Beijing 100049, P. R. China*

Xiaoxi Wu − *College of Materials Science and Opto-Electronic Technology & CAS Center for Excellence in Topological Quantum Computation & Key Laboratory of Vacuum Physics, University of Chinese Academy of Sciences, Beijing 100049, P. R. China*

Zijie Li − *College of Materials Science and Opto-Electronic Technology & CAS Center for Excellence in Topological Quantum Computation & Key Laboratory of Vacuum Physics, University of Chinese Academy of Sciences, Beijing 100049, P. R. China*

Qinqin Shi − *College of Materials Science and Opto-Electronic Technology & CAS Center for Excellence in Topological Quantum Computation & Key Laboratory of Vacuum Physics, University of Chinese Academy of Sciences, Beijing 100049, P. R. China*

Aidong Peng − *College of Materials Science and Opto-Electronic Technology & CAS Center for Excellence in Topological Quantum Computation & Key Laboratory of Vacuum Physics, University of Chinese Academy of Sciences, Beijing 100049, P. R. China*

Zhigang Shuai − *Department of Chemistry and MOE Key Laboratory of Organic Optoelectronics and Molecular Engineering, Tsinghua University, Beijing 100084, China;* ⓞ orcid.org/0000-0003-3867-2331

Huajie Chen − *Key Laboratory of Environmentally Friendly Chemistry and Application of the Ministry of Education, and Key Laboratory for Green Organic Synthesis and Application of Hunan Province, College of Chemistry, Xiangtan University, Xiangtan 411105, China;* ⓞ orcid.org/0000-0003-0366-8826

Complete contact information is available at:
https://pubs.acs.org/10.1021/acs.chemmater.0c00710

Author Contributions

The manuscript was written through contributions of all authors. All authors have given approval to the final version of the manuscript.

Notes

The authors declare no competing financial interest.

■ ACKNOWLEDGMENTS

■ REFERENCES

(1) Hung, L. S.; Chen, C. H. Recent progress of molecular organic electroluminescent materials and devices. *Mater. Sci. Eng., R* **2002**, *39*, 143−222.

(2) Wei, Q.; Fei, N.; Islam, A.; Lei, T.; Hong, L.; Peng, R.; Fan, X.; Chen, L.; Gao, P.; Ge, Z. Small-Molecule Emitters with High Quantum Efficiency: Mechanisms, Structures, and Applications in OLED Devices. *Adv. Opt. Mater.* **2018**, *6*, 1800512.

(3) Ostroverkhova, O. Organic optoelectronic materials: mechanisms and applications. *Chem. Rev.* **2016**, *116*, 13279−13412.

(4) Kido, J.; Kimura, M.; Nagai, K. Multilayer white light-emitting organic electroluminescent device. *Science* **1995**, *267*, 1332−1334.

(5) D'Andrade, B. W.; Forrest, S. R. White Organic Light-Emitting Devices for Solid-State Lighting. *Adv. Mater.* **2004**, *16*, 1585−1595.

(6) Farinola, G. M.; Ragni, R. Electroluminescent materials for white organic light emitting diodes. *Chem. Soc. Rev.* **2011**, *40*, 3467−3482.

(7) Wu, Z.; Ma, D. Recent advances in white organic light-emitting diodes. *Mater. Sci. Eng., R* **2016**, *107*, 1−42.

(8) Zhang, L.; Li, X.-L.; Luo, D.; Xiao, P.; Xiao, W.; Song, Y.; Ang, Q.; Liu, B. Strategies to Achieve High-Performance White Organic Light-Emitting Diodes. *Materials* **2017**, *10*, 1378.

(9) Sasabe, H.; Kido, J. Multifunctional Materials in High-Performance OLEDs: Challenges for Solid-State Lighting. *Chem. Mater.* **2011**, *23*, 621−630.

(10) Bates, F. S. Polymer-polymer phase behavior. *Science* **1991**, *251*, 898−905.

(11) Moons, E. Conjugated polymer blends: linking film morphology to performance of light emitting diodes and photodiodes. *J. Phys.: Condens. Matter* **2002**, *14*, 12235.

(12) Yang, X.; Loos, J. Toward high-performance polymer solar cells: the importance of morphology control. *Macromolecules* **2007**, *40*, 1353−1362.

(13) Tu, G. L.; Mei, C. Y.; Zhou, Q. G.; Cheng, Y. X.; Geng, Y. H.; Wang, L. X.; Ma, D. G.; Jing, X. B.; Wang, F. S. Highly Efficient Pure-White-Light-Emitting Diodes from a Single Polymer: Polyfluorene with Naphthalimide Moieties. *Adv. Funct. Mater.* **2006**, *16*, 101−106.

(14) Yang, Q.-Y.; Lehn, J.-M. Bright White-Light Emission from a Single Organic Compound in the Solid State. *Angew. Chem., Int. Ed.* **2014**, *53*, 4572−4577.

(15) Wang, L.; Lin, M.-F.; Wong, W.-K.; Cheah, K.-W.; Tam, H.-L.; Gao, Z.-Q.; Chen, C. H. Highly efficient white organic light-emitting diodes with single small molecular emitting material. *Appl. Phys. Lett.* **2007**, *91*, 183504.

(16) Fleetham, T.; Huang, L.; Li, J. Tetradentate Platinum Complexes for Efficient and Stable Excimer-Based White OLEDs. *Adv. Funct. Mater.* **2014**, *24*, 6066−6073.

(17) Williams, E. L.; Haavisto, K.; Li, J.; Jabbour, G. E. Excimer-Based White Phosphorescent Organic Light-Emitting Diodes with Nearly 100% Internal Quantum Efficiency. *Adv. Mater.* **2007**, *19*, 197−202.

(18) D'Andrade, B. W.; Brooks, J.; Adamovich, V.; Thompson, M. E.; Forrest, S. R. White Light Emission Using Triplet Excimers in Electrophosphorescent Organic Light-Emitting Devices. *Adv. Mater.* **2002**, *14*, 1032−1036.

(19) Mazzeo, M.; Vitale, V.; Della Sala, F.; Anni, M.; Barbarella, G.; Favaretto, L.; Sotgiu, G.; Cingolani, R.; Gigli, G. Bright White Organic Light-Emitting Devices from a Single Active Molecular Material. *Adv. Mater.* **2005**, *17*, 34−39.

(20) Kalinowski, J.; Cocchi, M.; Virgili, D.; Fattori, V.; Williams, J. A. G. Mixing of Excimer and Exciplex Emission: A New Way to Improve White Light Emitting Organic Electrophosphorescent Diodes. *Adv. Mater.* **2007**, *19*, 4000−4005.

(21) Angioni, E.; Chapran, M.; Ivaniuk, K.; Kostiv, N.; Cherpak, V.; Stakhira, P.; Lazauskas, A.; Tamulevičius, S.; Volyniuk, D.; Findlay, N. J.; Tuttle, T.; Grazulevicius, J. V.; Skabara, P. J. A single emitting layer white OLED based on exciplex interface emission. *J. Mater. Chem. C* **2016**, *4*, 3851−3856.

(22) Chen, Z.; Liu, X.-K.; Zheng, C.-J.; Ye, J.; Liu, C.-L.; Li, F.; Ou, X.-M.; Lee, C.-S.; Zhang, X.-H. High Performance Exciplex-Based Fluorescence-Phosphorescence White Organic Light-Emitting Device with Highly Simplified Structure. *Chem. Mater.* **2015**, *27*, 5206−5211.

(23) Singh, S. P.; Mohapatra, Y. N.; Qureshi, M.; Sundar Manoharan, S. White organic light-emitting diodes based on spectral broadening in electroluminescence due to formation of interfacial exciplexes. *Appl. Phys. Lett.* **2005**, *86*, 113505.

(24) Liu, B.; Nie, H.; Zhou, X.; Hu, S.; Luo, D.; Gao, D.; Zou, J.; Xu, M.; Wang, L.; Zhao, Z.; Qin, A.; Peng, J.; Ning, H.; Cao, Y.; Tang, B. Z. Manipulation of Charge and Exciton Distribution Based on Blue Aggregation-Induced Emission Fluorophors: A Novel Concept to Achieve High-Performance Hybrid White Organic Light-Emitting Diodes. *Adv. Funct. Mater.* **2016**, *26*, 776−783.

(25) Huang, J.; Nie, H.; Zeng, J.; Zhuang, Z.; Gan, S.; Cai, Y.; Guo, J.; Su, S.-J.; Zhao, Z.; Tang, B. Z. Highly Efficient Nondoped OLEDs with Negligible Efficiency Roll-Off Fabricated from Aggregation-Induced Delayed Fluorescence Luminogens. *Angew. Chem., Int. Ed.* **2017**, *56*, 12971−12976.

(26) Xu, B.; Wu, H.; Chen, J.; Yang, Z.; Yang, Z.; Wu, Y.-C.; Zhang, Y.; Jin, C.; Lu, P.-Y.; Chi, Z. White-light emission from a single heavy atom-free molecule with room temperature phosphorescence, mechanochromism and thermochromism. *Chem. Sci.* **2017**, *8*, 1909−1914.

(27) Yang, X.; Zhou, G.; Wong, W.-Y. Functionalization of phosphorescent emitters and their host materials by main-group elements for phosphorescent organic light-emitting devices. *Chem. Soc. Rev.* **2015**, *44*, 8484−8575.

(28) Evans, R. C.; Douglas, P.; Winscom, C. J. Coordination complexes exhibiting room-temperature phosphorescence: evaluation of their suitability as triplet emitters in organic light emitting diodes. *Coord. Chem. Rev.* **2006**, *250*, 2093−2126.

(29) Liu, B.; Li, X.-L.; Tao, H.; Zou, J.; Xu, M.; Wang, L.; Peng, J.; Cao, Y. Manipulation of exciton distribution for high-performance fluorescent/phosphorescent hybrid white organic light-emitting diodes. *J. Mater. Chem. C* **2017**, *5*, 7668−7683.

(30) Adamovich, V.; Brooks, J.; Tamayo, A.; Alexander, A. M.; Djurovich, P. I.; D'Andrade, B. W.; Adachi, C.; Forrest, S. R.; Thompson, M. E. High efficiency single dopant white electrophosphorescent light emitting diodes. *New J. Chem.* **2002**, *26*, 1171−1178.

(31) Ratzke, W.; Schmitt, L.; Matsuoka, H.; Bannwarth, C.; Retegan, M.; Bange, S.; Klemm, P.; Neese, F.; Grimme, S.; Schiemann, O.; Lupton, J. M.; Höger, S. Effect of Conjugation Pathway in Metal-Free Room-Temperature Dual Singlet-Triplet Emitters for Organic Light-Emitting Diodes. *J. Phys. Chem. Lett.* **2016**, *7*, 4802−4808.

(32) Chaudhuri, D.; Sigmund, E.; Meyer, A.; Röck, L.; Klemm, P.; Lautenschlager, S.; Schmid, A.; Yost, S. R.; Van Voorhis, T.; Bange, S.; Höger, S.; Lupton, J. M. Metal-Free OLED Triplet Emitters by Side-Stepping Kasha's Rule. *Angew. Chem., Int. Ed.* **2013**, *52*, 13449−13452.

(33) Ashraf, R. S.; Meager, I.; Nikolka, M.; Kirkus, M.; Planells, M.; Schroeder, B. C.; Holliday, S.; Hurhangee, M.; Nielsen, C. B.; Sirringhaus, H. Chalcogenophene comonomer comparison in small band gap diketopyrrolopyrrole-based conjugated polymers for high-performing field-effect transistors and organic solar cells. *J. Am. Chem. Soc.* **2015**, *137*, 1314−1321.

(34) McCulloch, Y.; Zhao, Z.; Zhao, W.; Ma, H.; Peng, Q.; He, Z.; Zhang, X.; Chen, Y.; He, X.; Lam, J. W. Y. Designing Efficient and Ultralong Pure Organic Room-Temperature Phosphorescent Materi-

als by Structural Isomerism. *Angew. Chem., Int. Ed.* **2018**, *57*, 7997−8001.

(35) Tang, P.; Okazaki, M.; Minakata, S.; Takeda, Y. Thermally activated delayed fluorescence vs. room temperature phosphorescence by conformation control of organic single molecules. *J. Mater. Chem. C* **2019**, *7*, 6616−6621.

(36) Zhang, T.; Gao, H.; Lv, A.; Wang, Z.; Gong, Y.; Ding, D.; Ma, H.; Zhang, Y.; Yuan, W. Z. Hydrogen bonding boosted the persistent room temperature phosphorescence of pure organic compounds for multiple applications. *J. Mater. Chem. C* **2019**, *7*, 9095−9101.

(37) Chen, C.; Huang, R.; Batsanov, A. S.; Pander, P.; Hsu, Y.-T.; Chi, Z.; Dias, F. B.; Bryce, M. R. Intramolecular charge transfer controls switching between room temperature phosphorescence and thermally activated delayed fluorescence. *Angew. Chem.* **2018**, *130*, 16645−16649.

(38) Ma, H.; Peng, Q.; An, Z.; Huang, W.; Shuai, Z. Efficient and long-lived room-temperature organic phosphorescence: theoretical descriptors for molecular designs. *J. Am. Chem. Soc.* **2018**, *141*, 1010−1015.

(39) Shuai, Z.; Peng, Q. Excited states structure and processes: Understanding organic light-emitting diodes at the molecular level. *Phys. Rep.* **2014**, *537*, 123−156.

(40) Duan, Y.-C.; Wen, L.-L.; Gao, Y.; Wu, Y.; Zhao, L.; Geng, Y.; Shan, G.-G.; Zhang, M.; Su, Z.-M. Fluorescence, Phosphorescence, or Delayed Fluorescence?-A Theoretical Exploration on the Reason Why a Series of Similar Organic Molecules Exhibit Different Luminescence Types. *J. Phys. Chem. C* **2018**, *122*, 23091−23101.

(41) Ma, H.; Shi, W.; Ren, J.; Li, W.; Peng, Q.; Shuai, Z. Electrostatic interaction-induced room-temperature phosphorescence in pure organic molecules from QM/MM calculations. *J. Phys. Chem. Lett.* **2016**, *7*, 2893−2898.

(42) Zhao, W.; Cheung, T. S.; Jiang, N.; Huang, W.; Lam, J. W.; Zhang, X.; He, Z.; Tang, B. Z. Boosting the efficiency of organic persistent room-temperature phosphorescence by intramolecular triplet-triplet energy transfer. *Nat. Commun.* **2019**, *10*, 1595.

(43) El-Sayed, M. A. Triplet state. Its radiative and nonradiative properties. *Acc. Chem. Res.* **1968**, *1*, 8−16.

(44) Shuai, Z.; Peng, Q. Organic light-emitting diodes: theoretical understanding of highly efficient materials and development of computational methodology. *Natl. Sci. Rev.* **2017**, *4*, 224−239.

(45) Yang, S.; Jiang, M. White light generation combining emissions from exciplex, excimer and electromer in TAPC-based organic light-emitting diodes. *Chem. Phys. Lett.* **2009**, *484*, 54−58.

(46) Tang, C. W.; VanSlyke, S. A.; Chen, C. H. Electroluminescence of doped organic thin films. *J. Appl. Phys.* **1989**, *65*, 3610−3616.